ChemistrySelect

Research Article
doi.org/10.1002/slct.202204543

Chemistry Europe
European Chemical Societies Publishing

www.chemistryselect.org

Design and Fabrication of Anticancer Drug-Loaded Poly(ε-caprolactone)-Poly(ethylene glycol)-Poly(ε-caprolactone) Micelles as Controlled Release System

Özlem Gökçe Kocabay*[a] and Osman İsmail[b]

In this study, doxorubicin (DOX) loaded polymeric micelles (PMs) were synthesized based on biodegradable poly(ε-caprolactone)-poly(ethylene glycol)-poly(ε-caprolactone) (PCEC) triblock copolymers. So four parameters (shaking speed (rpm) X_1, time of contact (hour) X_2, amount of triethylamine (TEA) (μL) X_3, DOX% X_4) were optimized. Then by adding valspodar (PSC 833) or D-α-Tocopherol polyethylene glycol 1000 succinate (TPGS 1000) to the formulations DOX/PSC 833-PMs or DOX/TPGS 1000-PMs were prepared by a nanoprecipitation method. The synthesized micelles exhibited high drug-loading encapsulation efficiency (>78.98%), high stability, and pH-dependent drug release. The results showed that the encapsulation efficiencies were not compromised by co-encapsulation of two agents. Finally, it was observed that the association of both DOX and PSC 833 or both DOX and TPGS 1000 within a single micelle formulation elicited the most soluble DOX as compared to DOX loaded formulations (DOX-PMs) while using a lower amount of polymer compared to separated micelle formulations.

Introduction

Polymeric micelles formed from the self-assembly of amphiphilic copolymers can promisingly increase the water solubility of anticancer drugs by 10- to 5000-fold. Polymeric micelles consist of two segments: the hydrophobic segment on the inside (core) and hydrophilic segment on the outside (shell). For this reason, the hydrophobic core may serve as a solubilisation storage for anticancer drugs with poorly water solubility. The hydrophilic shell supplies benefits containing longer blood stream period and increasing stability in the blood.[1] PCEC triblock copolymers are biocompatible, recyclable and easy to generate which showing encouraged applications in drug release systems.[2] Poly(ε-caprolactone) has several advantages, consisting of high crystallinity, low or no toxicity or side-effects, good compatibility with a lot of polymer compounds, and good level of biocompatibility. On the other hand, PCL easily crystallizes into crystals, which decreases its biodegradability. This characteristic limits PCL use as a carrier in the controlled drug delivery system. For this reason hydrophilic poly(ethylene glycol) (PEG) was incorporated into or blended with Poly(ε-caprolactone) to increase the hydrophilicity and the biodegradation rate.[3]

Doxorubicin hydrochloride (DOX·HCl) is an anthracycline drug. Doxorubicin hydrochloride (DOX·HCl), have been reported with a common uses in ovarium, breast and lung cancer as well as malignant lymphoma at the same time, the cardiotoxicity related side-effect restricts its long term use for such clinic aims. The disadvantages for example cardiac toxicity, short half-life and low solubility hinder the use of DOX.[4] The biologic and physicochemical properties of TPGS provide multi advantages for its applications in drug delivery such as high biocompatibility, enhancement of drug solubility, improvement of drug permeation and selective antitumor activity. Particularly, TPGS may inhibit the activity of ATP dependent P-glycoprotein and act as a potent excipient for overcoming multi-drug resistance (MDR) in tumor.[5] An important accumulation of DOX was determined in cells co-treated with PSC 833, when make comparison with cells treated only with DOX.[6]

Most of the time, the application of single-drug chemotherapy, also known as monotherapy, is inadequate to provide a comprehensive therapeutics plan which is effective in treating cancer. Consequently, attention has been directed toward planning drug delivery systems to co-deliver various combinations of therapeutics agents to overcome the disadvantages of single-drug chemotherapy.[7]

In previous work, we prepared PCEC polymeric micelles.[8] In the literature review, there is no study conducted with the DOX/PSC 833 or DOX/TPGS 1000 co-loaded PCEC drug delivery system. For this reason, this study is the first study to develop a formulation that will provide controlled drug release by using these active agents in the treatment of multiple drug resistant breast cancers. The first goal of present study is to identify the optimum parameters which control the efficiency of the elaboration process for synthesizing PCEC micelles loaded with DOX. The influences of (shaking speed (rpm) X_1, time of contact (hour) X_2, amount of TEA (μL) X_3, DOX% X_4) on DOX loading and encapsulation efficiency were evaluated in some detail. The "full factorial design" method was given preference herein.

[a] *Dr. Ö. Gökçe Kocabay*
Istanbul Restoration and Conservation Center and Regional Laboratory Directorate
T.R. Ministry of Culture and Tourism, Topkapı Palace, I. Courtyard, Bab-ı Hümayun Street, Sultanahmet, 34122 Istanbul, Turkey
E-mail: ozlemmgokce@hotmail.com
[b] *Assoc. Prof. Dr. O. İsmail*
Department of Chemical Engineering
Faculty of Chemical and Metallurgical Engineering
Yildiz Technical University, Davutpaşa Campus, 34210 Istanbul, Turkey

© 2023 Wiley-VCH GmbH

Check for updates

23656549, 2023, 4, Downloaded from https://chemistry-europe.onlinelibrary.wiley.com/doi/10.1002/slct.202204543 by Yildiz Teknik University, Wiley Online Library on [25/01/2023]. See the Terms and Conditions (https://onlinelibrary.wiley.com/terms-and-conditions) on Wiley Online Library for rules of use; OA articles are governed by the applicable Creative Commons License

The relationship of four parameters examined in this study is not available in the literature. And then the preparation and characterization of DOX loaded polymeric micelles (DOX-PMs) and co-loaded polymeric micelles (DOX/PSC 833-PMs and DOX/TPGS 1000-PMs) were investigated. Finally in vitro release and storage stability studies of these formulations carried out.

Experimental Section

Materials

Poly(ethylene glycol) (Molecular weight = 1450, 3350, 12000 g mol^{-1}) was purchased from Sigma and dried by azeotropic distillation using anhydrous toluene. ε-Caprolactone (CL) was purchased from Sigma and purified with calcium hydride (CaH_2) by vacuum distillation. Stannous octoate $Sn(Oct)_2$ was obtained from Sigma Aldrich and used as received. DOX-HCL was purchased from Sigma Aldrich. Valspodar (PSC 833) was purchased from Sigma. D-α- tocopheryl polyethylene glycol 1000 succinate (TPGS 1000) was obtained from Sigma. Tween 80 and sodium azide were obtained from Merck. Buffer solutions were obtained from Sigma. All other commercially available solvents and chemical agents were purchased from Merck Chemical Co. and used reagent grade without further purification. Cellulose dialysis membrane [molecular weight cut-off (MWCO) = 3.5 kDa] was obtained from Sigma-Aldrich, USA.

Full factorial design optimization of DOX-PMs

The PCEC triblock copolymer used at present work was synthesized by carrying out ring-opening copolymerization of ε-CL which was triggered by PEG using $Sn(Oct)_2$ as catalyst. The details can be found in our previous report. The DOX-PMs were synthesized by the nanoprecipitation method while the whole procedure was carried out in the dark. The PCEC copolymer used in this study was synthesized using PEG1450 at a feed ratio of ε-CL/PEG = 0.5. Due to the small size with narrow singular distribution monodispersed size distribution, zeta potential was in the desired range, and the polydispersity index was lower, drug encapsulation studies were focused on the micelles with the particle size of 225 nm, zeta potential of −2.2 mV and PDI of 0.75.[8]

The critical micelle concentration (CMC) is an efficient factor of micellar stability in addition to this a low critical value is required. The CMC is used to calculate the least formation concentration of the micelles in water. The CMC is an especially significant parameter for micelle-based drug release systems to prevent burst release upon injection into the blood stream. The CMC of the copolymer specifies at which point the micelles would disassemble upon dilution. As a result of the calculations, the CMC of the copolymer to be used for drug loading in this study was found to be 0.019202 mg mL^{-1}.[9]

The micelles showed narrow molecular weight distributions with a polydispersity index (PDI) of 1.15. The typical GPC curve of the PCEC copolymer to be used in the drug loading study is given in Figure 1.

According to Figure 1 only a sole peak existed, which indicated the mono-distribution of macromolecular weight and the nonexistence of any homopolymer, and furthermore implied that no trans-esterification or side reactions took place during copolymerization. The number average molecular weight and the weight average molecular weight of PCEC copolymer were 2521 and 2909 g mole^{-1}, respectively.[10]

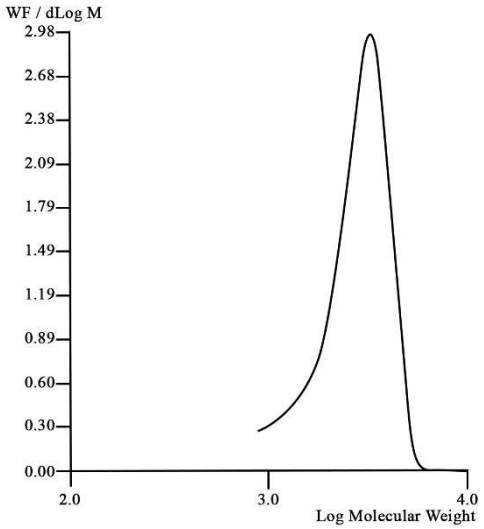

Figure 1. GPC curve of the synthesized PCEC copolymer.

For this multi-factor optimization, the traditional method of "changing a parameter at a time" could have been applied, but this way was avoided because it was tedious and did not guarantee to attain the optimal set of factors. Alternatively, the "full factorial design" method was preferred here. Based on a mathematical model of the combined effect of the processing parameters, this approach is known to be much more reliable.[11] So four parameters (shaking speed (rpm) X_1, time of contact (hour) X_2, amount of triethylamine (TEA) (μL) X_3, doxorubicin, DOX% X_4) were adjusted at two different values. For each of the $2^4 = 16$ experimental conditions, the experiments were replicated twice to obtain a reasonable average, DOX loading and encapsulation efficiency of the micelles were determined. Experimental error was calculated in the terms of standard deviation (SD). The average results were presented with ± SD value. The values of parameters are given in Table 1.

The "DOX%" (factor #4), was defined as the ratio of the weight of DOX with respect to the weight of PCEC in this solution. This ratio was adjusted to 2% (alternatively 5%). DOX.HCl was first neutralized to produce DOX-PMs. DOX.HCl in the amount of indicated in Table 1 was neutralized in 2 mL of acetone under magnetic stirring at 100 rpm whole night with TEA in the amount of stated in Table 1. The "amount of TEA" (factor #3) in this solution was equal to 22.5 μL (alternatively 45 μL). Then, in 4 mL of acetone, 90 mg of PCEC triblock copolymer was dissolved at 600 rpm for 1 hour, and the obtained this solution was added to the medicated solution. The resulting this organic solution was added dropwise by the help of a syringe to 15 mL of distilled water at 25 °C under magnetic stirring at 1000 rpm,[8] at the time of contact and shaking speed given in Table 1. The "shaking speed" (factor #1) was adjusted equal to 600 rpm (alternatively 1000 rpm). The period named as "time of contact" (factor #2) was adjusted equal to 1 hour (alternatively 3 hours). To remove untrapped DOX and TEA, and to produce micelles the mixture was then stirred for 24 hours. Acetone was removed by a rotary vacuum evaporator (BUCHI, R-200 Rotavapor and BUCHI V-800 Vacuum Controller) at 35 °C under descending pressure.

© 2023 Wiley-VCH GmbH

23656549, 2023, 4, Downloaded from https://chemistry-europe.onlinelibrary.wiley.com/doi/10.1002/slct.202204543 by Yildiz Teknik University, Wiley Online Library on [25/01/2023]. See the Terms and Conditions (https://onlinelibrary.wiley.com/terms-and-conditions) on Wiley Online Library for rules of use; OA articles are governed by the applicable Creative Commons License

23656549, 2023, 4, Downloaded from https://chemistry-europe.onlinelibrary.wiley.com/doi/10.1002/slct.202204543 by Yildiz Teknik University, Wiley Online Library on [25/01/2023]. See the Terms and Conditions (https://onlinelibrary.wiley.com/terms-and-conditions) on Wiley Online Library for rules of use; OA articles are governed by the applicable Creative Commons License

Table 1. Experimental design and observed responses.

Run number	X_1	X_2	X_3	X_4	Encapsulation efficiency (EE%)	Drug loading (%)
1	600	1	22.5	2:100	43.49 ± 3.15	0.97 ± 0.04
2	1000	1	22.5	2:100	50.27 ± 3.17	1.12 ± 0.09
3	600	3	22.5	2:100	52.90 ± 3.21	1.18 ± 0.11
4	1000	3	22.5	2:100	41.71 ± 4.06	0.93 ± 0.03
5	600	1	45	2:100	60.09 ± 1.87	1.33 ± 0.12
6	1000	1	45	2:100	54.05 ± 4.37	1.20 ± 0.11
7	600	3	45	2:100	47.17 ± 4.23	1.05 ± 0.05
8	1000	3	45	2:100	63.69 ± 3.58	1.41 ± 0.13
9	600	1	22.5	5:100	78.98 ± 3.42	4.25 ± 0.21
10	1000	1	22.5	5:100	73.92 ± 2.98	3.99 ± 0.03
11	600	3	22.5	5:100	77.89 ± 2.48	4.20 ± 0.19
12	1000	3	22.5	5:100	65.39 ± 1.35	3.55 ± 0.04
13	600	1	45	5:100	67.76 ± 2.64	3.67 ± 0.15
14	1000	1	45	5:100	56.67 ± 2.45	3.09 ± 0.17
15	600	3	45	5:100	70.97 ± 1.93	3.84 ± 0.18
16	1000	3	45	5:100	58.34 ± 1.92	3.18 ± 0.16

Table 2. Drug loading content, encapsulation efficiency, particle size, zeta potential and PDI values for DOX-PMs, PSC 833-PMs, TPGS 1000-PMs, DOX/PSC 833-PMs and DOX/TPGS 1000-PMs.

Type of drug	Amount of DOX (mg)	Amount of second agent (mg)	Drug loading content (%)	Encapsulation Efficiency (%)	Particle size (nm)	Zeta potential (mV)	PDI
DOX-PM	4.5	–	DOX:4.25	78.98	232	−6.5	0.383
PSC 833-PM	–	0.15	PSC 833:0.12	65.47	237	−4.3	0.291
	–	0.45	PSC 833:0.39	69.82	246	−4.0	0.264
DOX/PSC833-PM	4.5	0.45	DOX:4.28 PSC 833:0.40	79.47 70.54	277	−5.5	0.298
TPGS 1000-PM	–	0.15	TPGS 1000:*	*	230	−7.1	0.379
	–	0.45	TPGS 1000:*	*	235	−8.6	0.382
DOX/TPGS 1000-PM	4.5	0.45	DOX:4.43 TPGS 1000:*	82.36 *	227	−9.7	0.383

Fourier transform-infrared spectroscopy (FT-IR) analysis

The molecular structure of DOX, PCEC micelle, DOX-PCEC mixing, DOX-PMs were characterized by FT-IR (Shimadzu Corporation, IRPrestige21, Kyoto, JAPAN) using KBr pellets in the range of 4000–400 cm^{-1} wavelength region.

Preparation of DOX/PSC 833 and DOX/TPGS 1000 co-loaded micelles

Dual-drug loaded DOX/PSC 833-PMs and DOX/TPGS 1000-PMs were prepared only by adding PSC 833 or TPGS 1000 to the micelle components according to the method specified in "Full factorial design optimization of DOX-PMs" part. PSC 833 or TPGS 1000 was dissolved in acetone then this solution was added dropwise to distilled water under moderate mixing. To optimize drug encapsulation PSC 833 and TPGS 1000 (DOX:PSC 833 and/or DOX:TPGS 1000 ratio between 1:30 and 1:10) in different drug ratios were used with optimized DOX-PMs (Table 2).

Determination of particle size, polydispersity index and zeta potential of PMs

DOX-PMs, DOX/PSC 833-PMs and DOX/TPGS 1000-PMs were primarily dispersed in distilled water using dispersion. Particle size (Z-Ave), polydispersity index (PDI) and zeta potential (ζ) of the drug loaded PMs synthesized were determined using a Zetasizer Nano ZS (Malvern Instruments, Worcestershire, UK) equipped with 4.0 mV He–Ne laser (633 nm) along with photon correlation spectroscopy. The particle size was determined at 25 °C at a 90° scatter angle. The concentration of the all PMs was maintained at 1 mg mL^{-1}. Briefly, dried micelles were suspended in distilled water, vortexed to prevent particle aggregation and to provide uniform distribution of micelles. Data were evaluated based on volume distribution. Samples were analyzed three times and the average value was presented.

Evaluation of drug loading and encapsulation efficiency

Quantitative analysis was carried out by measuring the absorbance at 480 nm on a ultraviolet spectrophotometer (UV-Vis) (WTW Photolab) to compute the amount of DOX.[12] The mixture formulated in the preparation part of the PMs was centrifuged at 12000 rpm for 30 minutes (Thermo Scientific Heraeus Multifuge X3

© 2023 Wiley-VCH GmbH

FR Centrifuge Series). The supernatant was separated from the drug loaded PM. The supernatant was kept in the refrigerator at 4 °C. The amount of DOX loaded into PMs was determined by a subtraction method.[13] DL% and EE% were estimated according to equations (1) and (2):[14]

$$DL\% = ([\text{Total drug content}] - [\text{Free drug}])/([\text{Polymer}]+[\text{Total drug content}] - [\text{Free drug}])^{*}100 \quad (1)$$

$$EE\% = ([\text{Total drug content}] - [\text{Free drug}])/([\text{Total drug content}])^{*}100 \quad (2)$$

The quantitative analysis of PSC 833 and TPGS 1000 were determined using a validated HPLC method. Measurements were performed on a HPLC system (Shimadzu, Kyoto, Japan) equipped with chromatographic analysis pump (LC-20AT), auto-injector (SIL-20A HT), online degasser (DGU-20A_5) and column heater (CTO-10AS VP). HPLC method parameters for PSC 833 and TPGS 1000 analysis are shown in Tables 3 and 4, respectively.

Table 3. HPLC method parameters for PSC 833 analysis.

Column	Inertsil ODS 3 V C18 (250*4.6 5 μm)
Mobile Phase	ACN(50 %)–MeOH(50 %)
Flow Rate	1.5 mL min^{-1}
Column Temperature	50 °C
Wave Number	220 nm
Injection Volume	50 μL

Table 4. HPLC method parameters for TPGS 1000 analysis.

Column	Inertsil ODS 3 V C18 (250*4.6 5 μm)
Mobile Phase	ACN(65 %)–IPA(35 %)
Flow Rate	1.5 mL min^{-1}
Column Temperature	35 °C
Wave Number	220 nm
Injection Volume	10 μL

In vitro DOX release from DOX-PMs, DOX/PSC 833-PMs and DOX/TPGS 1000-PMs

In vitro DOX release from DOX-PMs was done by dialysis technique as described in our previous study.[10] DOX release from DOX/PSC 833-PMs and DOX/TPGS 1000-PMs also have been studied.

Stability of formulations

To evaluate the storage stability of DOX/PSC 833-PMs and DOX/TPGS 1000-PMs (40 mg) micelles were placed in pure water [containing 0.025 % (w/v) NaN_3] and kept at refrigerator temperature (5 °C) for a period of 15 days. At predetermined time intervals aliquots of samples were withdrawn and EE%, particle size and zeta potential of the PMs were determined.[8]

Results and Discussion

FT-IR analysis of DOX, PCEC PM and DOX-PMs

The chemical structures and probabilities of chemical and physical interactions of DOX, PCEC micelle, and the prepared DOX-PMs were characterized by FT-IR spectroscopy. Figure 2 shows the FT-IR spectra of them.

After removal of HCl, DOX.HCl was turned into a lipophilic molecule which was entrapped in the lipophilic nucleus of copolymeric micelles composed of amphiphilic triblock copolymer PCEC. The interaction between the DOX and micelle was investigated by FT-IR. These results show that there was no new chemical binding in DOX-PMs compared to free DOX (Figure 2a) and PCEC. DOX-micelle interactions only made some minor shifts in the characteristic peaks of the DOX and PCEC copolymer, which means that interactions are physical, for example Van Der Waals or hydrophobic interactions. The physical interaction between the DOX and PCEC did not make alteration of chemical structure of the DOX molecules and thereby the residual potential of the DOX. These results confirmed the chemical stability of the DOX, the sustainability of biological activities, and the probability of a sustained release system profile. Figure 2b shows that the peaks at 1107, 1246 cm^{-1} were assigned to the characteristic C–O–C stretching vibration of repeated $–OCH_2CH_2$ units of PEG and the stretching vibrations of the –COO– bonds, respectively. A similar result was obtained in the study of Feng et al. In the same study it was stated that the signals at 2944, 2866 cm^{-1} corresponded to the characteristic absorption of the C–H stretching bonds of $–CH_2CH_2$, which are similar to those of ε-CL. In this study, the peak values corresponding to these peaks were found as 2945 and 2868 cm^{-1}, respectively. Similarly, a weak peak at 1470 cm^{-1} may be due to $–CH_2$ bending vibration. The strong peak at 1725 cm^{-1} was due to carbonyl (C=O) adsorption.[15] In this study, these peak values were observed as 1471 and 1725 cm^{-1}, respectively. It was stated that the FT-IR spectrum of DOX exhibited multiple peaks at 3346, 2940, 2354 and 1072 cm^{-1}, which corresponded to the different quinine and ketone carbonyls in DOX. Nevertheless, it was pointed out that it cannot be delineated the specific bonds between specific quinine and ketone because they both have carbonyl groups.[16] In this study, these peaks corresponded to 3342, 2940, 2360, and 1072 cm^{-1}, respectively. For DOX, characteristic bands at 1630 cm^{-1} that corresponding to N–H bending vibrations were observed at 1617 cm^{-1}, characteristic bands at 1427 cm^{-1} that corresponding to C–C stretching vibrations were observed at 1409 cm^{-1}, characteristic bands at 1010 cm^{-1} that corresponding to C–O stretching vibration were observed at 1006 cm^{-1}. Nassar et al. stated that the FT-IR spectrum of DOX showed multiple peaks at 1730 (C–O) and 1577 cm^{-1} (N–H).[17] It was expressed that C–H and C=C vibrations of benzene ring, on DOX, correspond to 793 cm^{-1} and a = C–H out of plane bending was also observed at 758 and 700 cm^{-1}.[18] These peaks mentioned were also obtained in this study as 795, 763 and 707 cm^{-1}, respectively. These peaks were also found in the FT-IR spectrum of DOX-PMs. The appearance of these characteristic bands has proven that DOX

© 2023 Wiley-VCH GmbH

23656549, 2023, 4, Downloaded from https://chemistry-europe.onlinelibrary.wiley.com/doi/10.1002/slct.202204543 by Yildiz Teknik University, Wiley Online Library on [25/01/2023]. See the Terms and Conditions (https://onlinelibrary.wiley.com/terms-and-conditions) on Wiley Online Library for rules of use; OA articles are governed by the applicable Creative Commons License

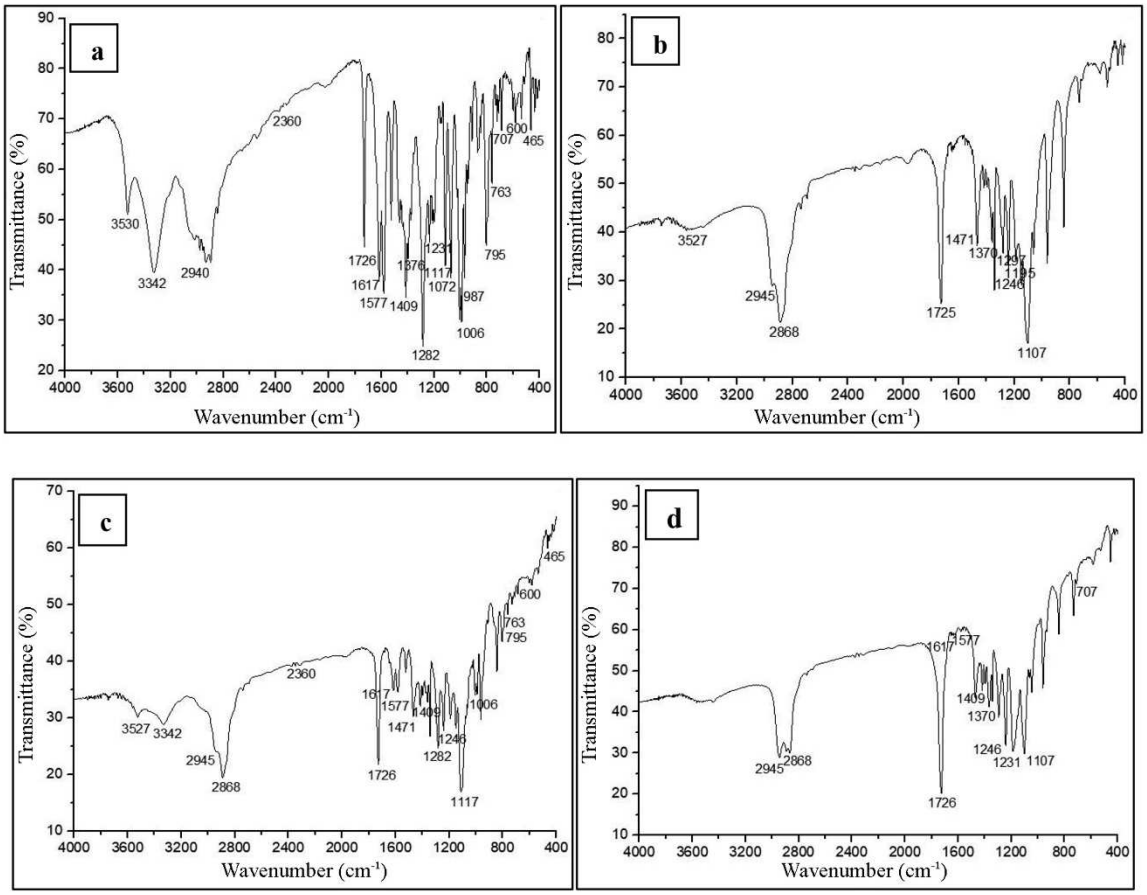

Figure 2. FT-IR spectrum: a. DOX, b. PCEC micelle, c. DOX-PCEC mixing, d. DOX loaded PCEC micelle.

has miscibility with the PCEC PM (Figure 2c) moreover DOX was successfully loaded to the DOX-PM (Figure 2d) system. Three peaks at 1726, 1409 and 707 cm^{-1} belonging to the DOX were observed in the DOX-PM spectrum but their intensity decreased. The FT-IR spectra corresponding to the DOX-PMs exhibited the characteristic bands of both contents (DOX and PCEC) without any spectral shift in either band.

The effect of experimental factors on encapsulation efficiency

The graphs in Figures 3–6 show the evolution of the mean value of EE on these factors from minimum to maximum values.

Figure 3 EE(X_1) shows that the EE significantly decreases with increasing shaking speed. For example, under the experimental conditions where the time of contact was 1 hour, the amount of TEA was 45 μL, the DOX% was 5:100, the EE decreased from 67.76 ± 2.64 to 56.67 ± 2.45 % when the shaking speed increased from 600 to 1000 rpm. The shaking speed of the dispersive process is an important parameter affecting the morphology of the micelles. Furthermore, Yasin et al. stated that the microspheres particle size decreased gradually with the increase of shaking speed. Correlating these

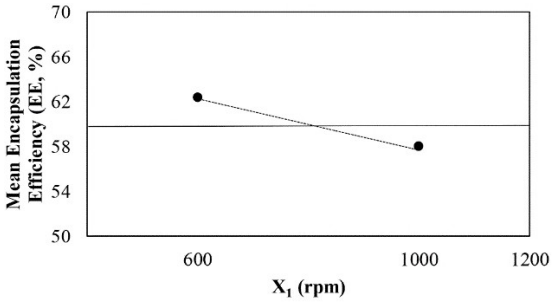

Figure 3. Influence of the shaking speed X_1 on the mean value of EE.

results indicated that the bigger the microparticles, the larger EE. The reason is that higher agitating speed which provided stronger shear force leading to the formation of smaller droplets and consequently smaller microspheres.[19] For this reason as shown in Table 1, optimized production factors can be obtained at a shaking speed of 600 rpm. The data obtained as a result of the equation showed that X_4 (drug:polymer ratio) was more important than X_1 (shaking speed). At the time of homogenization of 10 min the EE% for the stirring rate of 15000, 12000 and 10000 rpm were 79.1 ± 1.76, 83.5 ± 1.09 and 87.3 ± 2.5, respectively. Enin et al. stated that the negative sign

© 2023 Wiley-VCH GmbH

23656549, 2023, 4, Downloaded from https://chemistry-europe.onlinelibrary.wiley.com/doi/10.1002/slct.202204543 by Yildiz Teknik University, Wiley Online Library on [25/01/2023]. See the Terms and Conditions (https://onlinelibrary.wiley.com/terms-and-conditions) on Wiley Online Library for rules of use; OA articles are governed by the applicable Creative Commons License

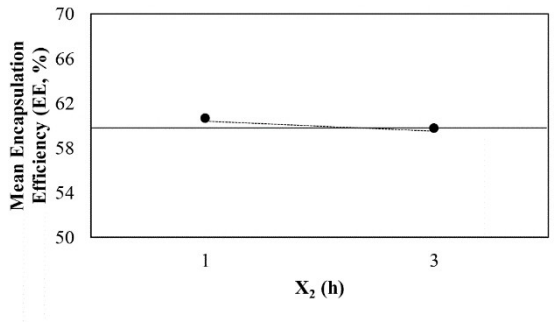

Figure 4. Influence of the time of contact X_2 on the mean value of EE.

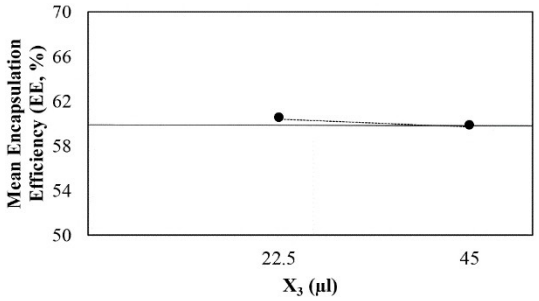

Figure 5. Influence of the amount of TEA X_3 on the mean value of EE.

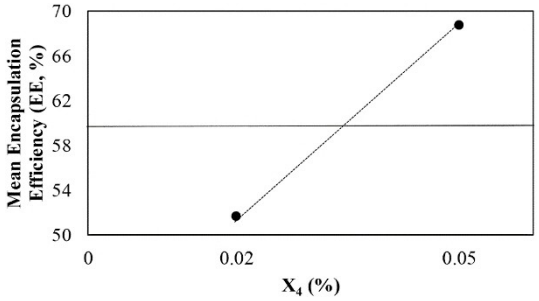

Figure 6. Influence of the DOX% X_4 on the mean value of EE.

of stirring rate indicates a significant antagonistic effect on EE %. Increasing stirring rate decreases the entrapping of quercetin into nanoemulsions particles by reducing their contact.[20]

Figure 4 EE(X_2) shows that the EE follows a small, although significant, decrease with increasing time of contact. Under the experimental conditions where the shaking speed was 600 rpm, the amount of TEA was 45 µL, DOX% was 2:100, the EE decreased from 60.09 ± 1.87 to 47.17 ± 4.23% when the time of contact increased from 1 hour to 3 hours. According to the literature, this probably means that a process with longer time of contact leads to smaller microparticles. While the PVA content was 0.60%, polysaccharides concentration was 11.0 µg mL^{-1}, stirring speed was 11000 rpm, the encapsulation efficiency decreased from 61.77 to 60.39% when the stirring time increased from 1.5 to 2.5 min.[21]

Figure 5 shows that the variation of the amount of TEA has nearly no effect on the EE. Under the experimental conditions where the shaking speed was 1000 rpm, time of contact was 1 hour, DOX% was 2:100, the EE increased by a narrow margin from 50.27 ± 3.17 to 54.05 ± 4.37% when the amount of TEA was increased from 22.5 to 45 µL. Zhu et al. reported that EE of DOX increased with the amount of TEA increasing. It was stated that when DOX.HCl was encapsulated within nanoparticles without using TEA, little DOX was incorporated into nanoparticles, owing to the hydrophilicity of its protonated form. When the addition volume of TEA increased, the removal of hydrochloride from DOX.HCl was promoted, therefore, the higher hydrophobicity of DOX was considered to allow physical entrapment in a more efficient manner by hydrophobic interaction. Accordingly, when 20, 50, 100 and 165 µL of TEA were used, the EE were found as 15.44 ± 1.11, 49.30 ± 1.75, 70.07 ± 1.62 and 86.71 ± 2.05%, respectively.[22]

Figure 6 EE(X_4), shows that the EE exhibits a very important increase when increasing the DOX concentration. Under the experimental conditions where the shaking speed was 600 rpm, time of contact was 1 hour, the amount of TEA was 22.5 µL the EE increased from 43.49 ± 3.15 to 78.98 ± 3.42% when the DOX% increased from 2:100 to 5:100. The EE of prodigiosin (PG) increased with increasing drug:polymer ratio, with S4 (concentration of the drug: 5 mg mL^{-1}) having a percentage encapsulation of 90 ± 4% and S1 (concentration of the drug: 1 mg mL^{-1}) a percentage encapsulation ratio of 66.7 ± 3.3%.[23] Shivhare et al. pointed out that as the ratio of drug-to-polymer increased, EE increased; this is due to the fact that higher ratio of drug-to-polymer would produce large size droplets with decreased surface area, such that diffusion of drug from such microsphere will be slow, resulting in higher EE.[24]

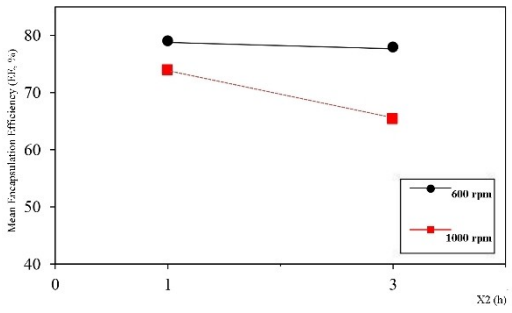

Figure 7. Interaction plots of the X_1–X_2 experimental factors on the encapsulation efficiency, the solid lines correspond to the low level of the factors and the dashed lines to their high level.

Figures 7–12 show the interaction plots of shaking speed, time of contact, the amount of TEA, and the percentage of DOX on the EE.

As can be seen in Figures 7–12, there is no significant interactions between shaking speed vs. time of contact,

© 2023 Wiley-VCH GmbH

23656549, 2023, 4, Downloaded from https://chemistry-europe.onlinelibrary.wiley.com/doi/10.1002/slct.202204543 by Yildiz Teknik University, Wiley Online Library on [25/01/2023]. See the Terms and Conditions (https://onlinelibrary.wiley.com/terms-and-conditions) on Wiley Online Library for rules of use; OA articles are governed by the applicable Creative Commons License

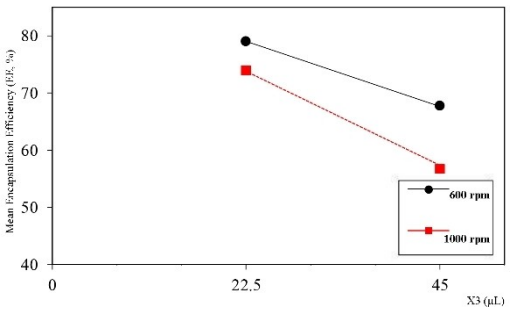

Figure 8. Interaction plots of the X_1–X_3 experimental factors on the encapsulation efficiency, the solid lines correspond to the low level of the factors and the dashed lines to their high level.

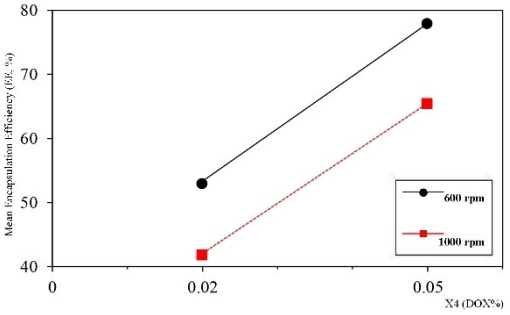

Figure 9. Interaction plots of the X_1-X_4 experimental factors on the encapsulation efficiency, the solid lines correspond to the low level of the factors and the dashed lines to their high level.

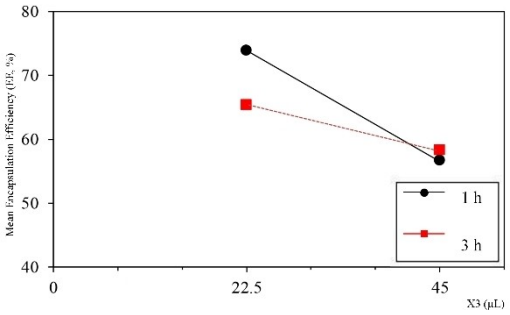

Figure 10. Interaction plots of the X_2–X_3 experimental factors on the encapsulation efficiency, the solid lines correspond to the low level of the factors and the dashed lines to their high level.

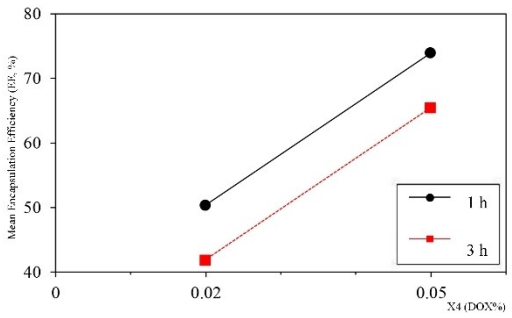

Figure 11. Interaction plots of the X_2–X_4 experimental factors on the encapsulation efficiency, the solid lines correspond to the low level of the factors and the dashed lines to their high level.

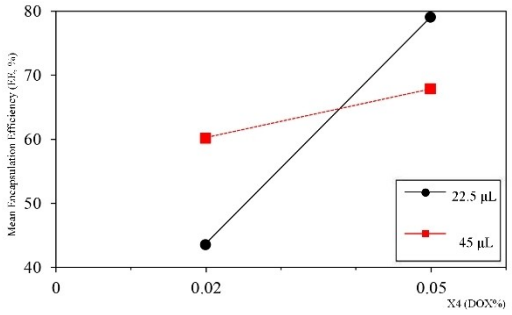

Figure 12. Interaction plots of the X_3–X_4 experimental factors on the encapsulation efficiency, the solid lines correspond to the low level of the factors and the dashed lines to their high level.

shaking speed vs. amount of TEA, time of contact vs. amount of TEA, and time of contact vs. DOX%. On the other hand the interactions between shaking speed vs. DOX%, and between amount of TEA vs. DOX% were significant because DOX% had a great influence on EE. For the interaction between shaking speed vs. DOX%: At the high level of DOX%, the response EE on a large scale decreases as the shaking speed goes from low to high level. But at the lower level of the DOX%, this decrease is lesser pronounced. For the interaction between amount of TEA vs. DOX%: At the high level of DOX%, the response EE substantially decreases as the amount of TEA goes from low to high level. Nevertheless, at the lower level of the DOX%, the response EE increases majorly.

According to results obtained $X_1 = 600$ rpm, $X_2 = 1$ hour, $X_3 = 22.5$ µL and $X_4 = 5\%$ were determined as the optimum factors. The EE calculated under these optimum conditions is $78.98 \pm 3.42\%$.[8]

Evaluation of drug loading data of DOX-PMs

Based on the Equation (1), the DL content was calculated and presented in Table 1. To give an example under the experiment conditions where the time of contact was 3 hours, amount of TEA was 45 µL and DOX% was 2:100 the DL value increased from 1.05 to 1.41% when the shaking speed increased from 600 to 1000 rpm. The DL generally reduced by increasing the shaking speed from 600 to 1000 rpm, the reason is that the possibility of diffusion of the DOX to the outer phase and during solvent removal at a higher rate rapid diffusion can occur (Table 1). In this study, theoretical DL was chosen as 2 and 5%. DL showed a reasonable increase with an increase in the proportion of DOX (Table 1). When the concentrations of the prodigiosin were 1, 1.5, 2 and 5 mg mL^{-1}, drug loading capacity (%) values were calculated as 6.7 ± 0.3, 12 ± 0.6, 15.3 ± 0.8 and 45 ± 2.3, respectively.[23]

© 2023 Wiley-VCH GmbH

23656549, 2023, 4, Downloaded from https://chemistry-europe.onlinelibrary.wiley.com/doi/10.1002/slct.202204543 by Yildiz Teknik University, Wiley Online Library on [25/01/2023]. See the Terms and Conditions (https://onlinelibrary.wiley.com/terms-and-conditions) on Wiley Online Library for rules of use; OA articles are governed by the applicable Creative Commons License

Particle size distribution, zeta potential and polydispersity index of DOX-PMs, DOX/PSC 833-PMs and DOX/TPGS 1000-PMs

Table 2 provides particle size, zeta potential and PDI values for DOX-PMs, PSC 833-PMs, TPGS 1000-PMs, DOX/PSC 833-PMs and DOX/TPGS 1000-PMs.

The particle size, zeta potential and PDI value for DOX-PMs synthesized by using optimum factors and that providing highest EE were found as 232 nm, −6.5 mV and 0.383, respectively.[8] The DOX loading did not significantly affect the size of the PMs and did not change the size distribution of the PMs. A similar result was observed in a study done by Cavalcante et al.[25] Figure 13 shows particle size distribution and zeta potential graphs of the DOX-PMs synthesized by using optimum factors and that providing highest EE.

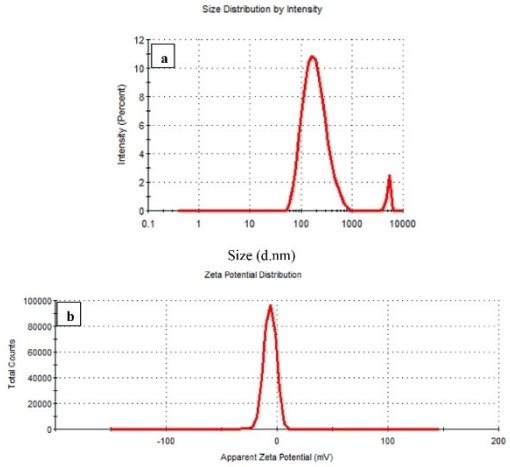

Figure 13. Particle size distribution and zeta potential of micelle synthesized by using optimum factors and that providing highest encapsulation efficiency: a. particle size distribution, b. zeta potential.

The PDI value suggested that the obtained DOX-PMs were monodispersed and did not aggregate in water. DOX-PMs were negatively charged. This may increase the circulation time of the drug. Surface charge is important in determining whether the nanoparticles will cluster in blood flow or will adhere to or interact with the oppositely charged cell membrane. The plasma and blood cells always had a negative charge; nanoparticles with slight negative surface charge may minimize nonspecific interactions with these components through electrostatic interactions.[8]

DOX/PSC 833-PMs and DOX/TPGS 1000-PMs showed unimodal and narrow size distribution. The size of all drug loaded PMs were suitable for EPR effect to achieve passive targeting. The PDI value of PSC 833-PM containing 0.15 and 0.45 mg PSC 833 were 0.291 and 0.264, respectively. The PDI value of DOX/PSC 833-PM containing 0.45 mg PSC 833 and 4.5 mg DOX was 0.298. The PDI value of TPGS 1000-PM containing 0.15 and 0.45 mg TPGS 1000 were 0.379 and 0.382, respectively. The PDI value of DOX/TPGS 1000-PM containing 0.45 mg TPGS 1000 and 4.5 mg DOX was 0.383. The mean particle size of the PMs with different drug types and quantities had an acceptably good polydispersity allowing diffusion into malignant tissue via gaps present in the highly permeable tumor blood vessels. Zeta potential values were between (−4.0)–(−9.7) mV. The particle size of TPGS 1000-PM containing 0.15 and 0.45 mg TPGS 1000 were 230 and 235 nm, respectively. The size of DOX/TPGS 1000-PM was 227 nm. The particle size of DOX/TPGS 1000-PM was found smaller than DOX-PM, which may be due to the more hydrophobic interaction between DOX and the micelle core.[26] The particle size of PSC 833-PM containing 0.15 and 0.45 mg PSC 833 were 237 and 246 nm, respectively. The size of the PM arising from the co-loading of 4.5 mg DOX and 0.45 mg PSC 833 was 277 nm. It is thought that dual drug loading may be responsible for this small size growth. The increase in particle size also showed successful DL in PMs. Also, the dual drug loaded particle properties have been shown to be similar to single agent loaded PMs which can be attributed to small amounts of chemosensitizer (e.g., 0.15 or 0.45 mg loading) in the PMs.

Encapsulation efficiency and drug loading content of DOX/PSC 833 or DOX/TPGS 1000 co-loaded PMs

Combination therapy, a treatment manner which combines two or more therapeutics drugs, is a cornerstone of cancer treatment. The combination of anticancer agents improves efficiency in comparison with the monotherapy approach because it targets key pathways in a characteristically synergistic or an additive manner.[27] In this study, PSC 833 or TPGS 1000 agents were co-loaded with DOX into PMs to obtain PMs with the highest EE% of DOX. In this study, it was focused on reducing the required dose of DOX in chemotherapy through the synergistic effect of PSC 833 or TPGS 1000 with DOX. Table 2 provides drug loading content and encapsulation efficiency values for DOX-PMs, PSC 833-PMs, TPGS 1000-PMs, DOX/PSC 833-PMs and DOX/TPGS 1000-PMs.

From Table 2 the observed responses were reproducible and consistent with the predicted values. When using 4.5 mg of DOX, DOX loading were calculated as 4.25, 4.28 and 4.43% for DOX-PM, DOX/PSC 833-PM and DOX/TPGS 1000-PM, respectively. PSC 833 loading in PSC 833-PM were found as 0.12 and 0.39% for 0.15 and 0.45 mg loading, respectively. The PSC 833 loading was found to be 0.40% in the DOX/PSC 833-PM which consisting of 4.5 mg DOX and 0.45 mg PSC 833 loading. The amount of TPGS 1000 remaining in the supernatant was very low. As a result, loading content and EE of TPGS 1000 could not be accurately measured by high performance liquid chromatography (HPLC). The experiments and results showed that DL can be easily controlled by changing the feed concentration of DOX, PSC 833, and TPGS 1000. As a result, their ratios can be completely controlled. The loading capacity of the two drugs with adjustable ratio has shown that this release system is a flexible multimodality therapy against cancer.

© 2023 Wiley-VCH GmbH

23656549, 2023, 4, Downloaded from https://chemistry-europe.onlinelibrary.wiley.com/doi/10.1002/slct.202204543 by Yildiz Teknik University, Wiley Online Library on [25/01/2023]. See the Terms and Conditions (https://onlinelibrary.wiley.com/terms-and-conditions) on Wiley Online Library for rules of use; OA articles are governed by the applicable Creative Commons License

It can be easily seen from Table 2 that EE was closely related to the type and amount of drug. PSC 833 is a more hydrophobic derivative of CyA and therefore it is compatible with the hydrophobic micellar core (PCL).[28] Based on a better compatibility between the PSC 833 and PCL, the PSC 833 is expected to remain at higher rate relation with the PCEC PMs. In the formulation containing 0.45 mg PSC 833 and 4.5 mg DOX, the EE values of DOX and PSC 833 were 79.47 and 70.54 %, respectively. In the PSC 833-PMs containing 0.15 and 0.45 mg PSC 833, the EE values of the PSC 833 were 65.47 and 69.82 %, respectively. Ouahab et al. observed that physical entrapment of hydrophobic drugs in PMs was driven by the hydrophobic interactions between drugs and hydrophobic segments of mPEG-PLA polymer. In general, it has been stated that drug hydrophobicity played a decisive role in the drug loading process. A similar result was obtained in this study. The higher loading and stability is due to the difference of distribution of the drugs in the core according to their partition coefficient.[29] Without the solubilization of TPGS 1000, the EE value of the DOX in the core of PMs was 78.98 %, which was slightly lower than PMs with TPGS 1000 modification. In the formulation containing TPGS 1000 and DOX the EE value of DOX was 82.36 %.

The results showed that high encapsulation and loading efficiency values were obtained in this study for DOX/PSC 833-PMs and DOX/TPGS 1000-PMs. The high EE of DOX, PSC 833 and TPGS 1000 may be related to the high affinity for PMs. In addition, high loading efficiency values indicate other advantages of this advanced release system, in other words a low amount of carrier is required for effective drug release.

In vitro release of DOX from DOX-PMs, DOX/PSC 833-PMs and DOX/TPGS 1000-PMs

Figure 14 shows the in vitro DOX release from DOX.HCl, DOX-PMs, DOX/PSC 833-PMs and DOX/TPGS 1000-PMs for 24 hours.

In vitro release profile of DOX from DOX/TPGS 1000-PM and DOX/PSC 833-PM showed a sustained biphasic release for up to 24 hours with a very small initial burst release (Figures 14a–b). The burst effect is defined here as the percentage released in the first 2 hours compared to the total released DOX, because all PM samples showed an obvious DOX release in the first 2 hours. All samples had a burst release effect due to the surface absorption of the PMs. At pH 7.4 the burst effect of DOX-PM, DOX/TPGS 1000-PM and DOX/PSC 833-PM were 17, 17 and 13 %, respectively and these generally increased with decreasing pH.

In vitro release behavior of DOX from PMs at 37 °C was investigated by dialysis method at pH 7.4 mimicking the normal body blood and under tumoral extracellular environment (pH 6.5) and under endo/lysosome mimic conditions (pH 5.0).[30] PMs were tight at pH 7.4 (Figure 14c), DOX release was slow and sustainable, then DOX release profiles reached a plateau. Since DOX was not released in the medium, it was assumed that the plateau phase was reached by sampling after 24 hours of release study. This showed that DOX-PMs retain their micelle structure under physiological conditions and

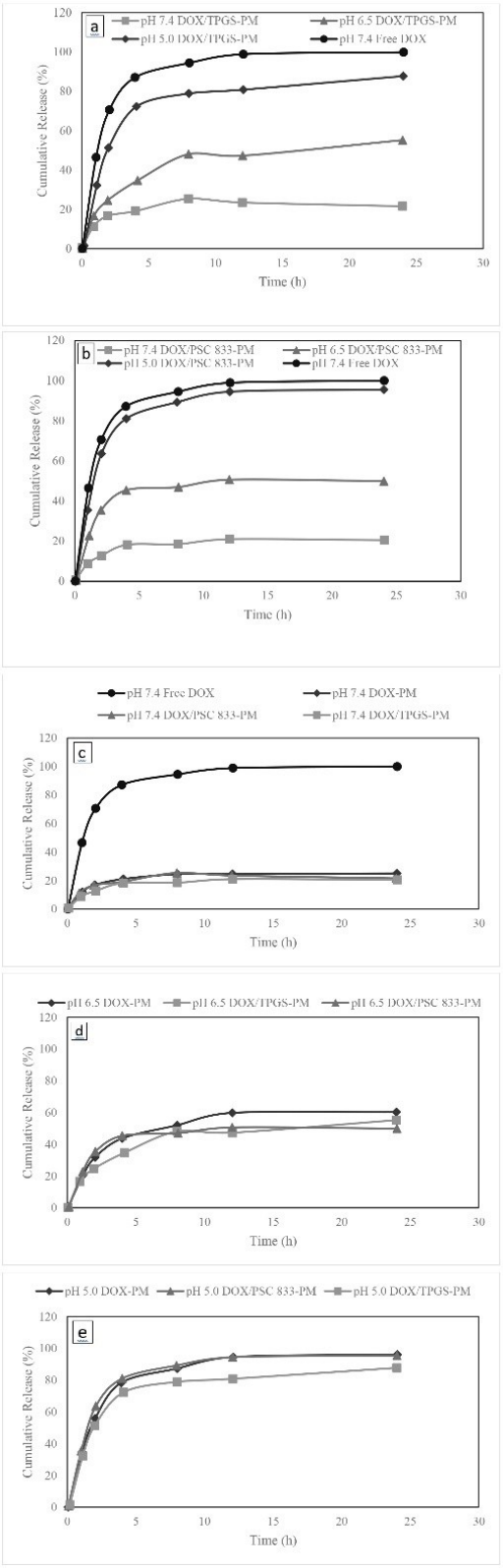

Figure 14. In vitro DOX release from PMs in PBS medium with different pH values at 37 °C: a. DOX/TPGS 1000-PM, b. DOX/PSC 833-PM, c. pH 7.4, d. pH 6.5, e. pH 5.0.

© 2023 Wiley-VCH GmbH

23656549, 2023, 4, Downloaded from https://chemistry-europe.onlinelibrary.wiley.com/doi/10.1002/slct.202204543 by Yildiz Teknik University, Wiley Online Library on [25/01/2023]. See the Terms and Conditions (https://onlinelibrary.wiley.com/terms-and-conditions) on Wiley Online Library for rules of use; OA articles are governed by the applicable Creative Commons License

exhibit appropriate stability during systematic circulation. As shown in Figure 14c, during the initial 2 hours approximately 17, 13 and 17% of DOX were released from DOX-PM, DOX/TPGS 1000-PM and DOX/PSC 833-PM, respectively. After that, DOX release profiles reached a plateau. For 24 hours, approximately 25 (DOX-PM), 21 (DOX/TPGS 1000-PM) and 22% (DOX/PSC 833-PM) of DOX were released from PMs. Which means that at least 75–80% of DOX may be protected from enzyme degradation or hydrolytic degradation. However, under these conditions, the strong hydrophobic interactions between DOX molecules themselves as well as between DOX and the micelles probably contributed to the retaining of most of the drug in the micelles.[31] However, DOX release at pH 6.5 accelerated compared to pH 7.4. As shown in Figure 14d, during the initial 2 hours approximately 32, 25 and 35% of DOX were released from DOX-PM, DOX/TPGS 1000-PM and DOX/PSC 833-PM, respectively. After that, DOX release profiles reached a plateau. For 24 hours, approximately 60 (DOX-PM), 55 (DOX/TPGS 1000-PM) and 50% (DOX/PSC 833-PM) of DOX were released from PMs. Although the DOX release rate was much faster than pH 6.5, a similar situation was observed at pH 5.0 (Figure 14e). This has proved that PMs are loose and/or unstable at low pH conditions and DOX release is extremely accelerated. During the initial 2 hours, approximately 56, 51 and 64% of DOX were released from DOX-PM, DOX/TPGS 1000-PM and DOX/PSC 833-PM, respectively. After that, DOX release profiles reached a plateau. After 24 hours, the DOX released from DOX-PM and DOX/PSC 833-PM were 96 and 95%, respectively, while these values were higher than DOX released from DOX/TPGS 1000-PM (88%). As expected, the release of DOX from the two PM systems showed distinct pH dependence and was gradually accelerated with decreasing pH (Figures 14a–b). A similar result was obtained in the study of Akyol and Senol.[32] Similar release patterns were observed at the same pH for all PMs (Figures 14c–e). Mentioned faster release of DOX in acidic conditions was also observed by Kataoka and coworkers with the DOX-loaded PEG-PBLA copolymer micelles, and is likely due to the re-protonation of the amino group of DOX and faster degradation of micelle core at lower pH.[29] The DOX release profiles of the co-delivery system were similar to the release profile of DOX alone in the release system. Compared to DOX-PM, the mixture obtained by adding PSC 833 (DOX/PSC 833-PM) did not affect DOX release at pH 5.0–7.4 (Figures 14c–e). Incorporating of TPGS 1000 (DOX/TPGS 1000-PM) slowly weakened the stabilization of the PM at pH 5.0 (Figure 14e) while maintaining stability of the PM at pH 6.5 (Figure 14d) and pH 7.4 (Figure 14c). The PM was able to control DOX release and DOX, TPGS 1000 and PSC 833 did not affect release behavior of each other. In this study, even with the lowest release rate sample DOX/TPGS 1000-PM, approximately 22% of the total loaded DOX was separated from PMs within 24 hours. Emami et al. stated that the incorporation of α-TS (part of TPGS) into the TS-CS micelles enhanced hydrophobic interaction between PTX and the core of micelles to form a tightly packed hydrophobic core.[26] Also the results obtained in this study showed that the incorporation of TPGS 1000 and/or PSC 833 into the PMs were enhanced the DOX solubility.

As seen in Figures 14a–c in vitro DOX release from DOX-PM, DOX/TPGS 1000-PM and DOX/PSC 833-PM was more sustainable than the free DOX solution. For example, while almost all of the free DOX was released within 24 hours, DOX-PM, DOX/TPGS 1000-PM and DOX/PSC 833-PM released only 25, 22 and 21% of DOX, respectively.

Biodegradation of PCL is slow and may require years (for example 1–2 years) for whole bioresorption[33] therefore, this synthesized PM is not expected to degrade significantly over the time frame of this study. Regarding the structure of the synthesized amphiphilic copolymer micelles, the release rate of the drug is controlled by both the rate of hydrolysis of the ester bond between the copolymer and the drug and the rate of diffusion.[34] In this study, DOX made a rapid release in the first two hours. At this stage, the diffusion mechanism can play a big role. Similarly, according to the dissolution principle, the PMs showed a core-shell morphology with a hydrophobic core surrounded by a hydrophilic PEG shell. DOX, a hydrophobic drug, showed greater loading in the hydrophobic core, but the part of the drug at the superficial layers of polymeric micelles dissolved and caused the first accelerated release that is more easily diffused.[35] Afterwards, the release speed of DOX slowed down which might be due to degradation of micelles, instead of diffusion, takes the major role in this stage. The release rate of DOX after 12 hours was very slow, but the release continued anyway. Subsequent release showed that the inner DOX did not dissolve easily due to stronger loading in the core, solution permeation and copolymer degradation, which prevented swelling and thus diffusion of the drug. The subsequent sustainable release showed that DOX can be kept stable in the micelle core before slow release by drug diffusion. A similar observation was made in study of Liu et al.[36]

Stability study of PMs

In view of the potential utility of nanoparticles (NPs) formulation for pharmaceutical applications, stability of EE, size and zeta potential is significant for long-term storage, transportation, and scalable processing.[37] For this reason, the stability of the PMs was determined for a period of 15 days in this study. Table 5 shows physical and chemical stability data of various PM formulations at refrigerator temperature (5 °C).

As given in Table 5, EE values of DOX for DOX/TPGS 1000-PM and DOX/PSC 833-PM showed a slight decrease from 82.36 to 78.63% and from 79.47 to 75.12%, respectively. However, these differences are not an important change. Similarly, EE values of PSC 833 for PSC 833-PM and DOX/PSC 833-PM did not change significantly, although a slight decrease was observed from 69.82 to 65.93% and from 70.54 to 66.02%, respectively.

Mean diameters of TPGS 1000-PM, DOX/TPGS 1000-PM, PSC 833-PM and DOX/PSC 833-PM increased from 235 to 247 nm, from 227 to 240 nm, from 246 to 256 nm, from 277 to 292 nm, respectively. The size of all PMs increased slightly throughout the measurement period. No visible aggregation occurred in the system during storage. This observation cannot be a sign of aggregation, which usually leads to several fold increases.

© 2023 Wiley-VCH GmbH

23656549, 2023, 4, Downloaded from https://chemistry-europe.onlinelibrary.wiley.com/doi/10.1002/slct.202204543 by Yildiz Teknik University, Wiley Online Library on [25/01/2023]. See the Terms and Conditions (https://onlinelibrary.wiley.com/terms-and-conditions) on Wiley Online Library for rules of use; OA articles are governed by the applicable Creative Commons License

23656549, 2023, 4, Downloaded from https://chemistry-europe.onlinelibrary.wiley.com/doi/10.1002/slct.202204543 by Yildiz Teknik University, Wiley Online Library on [25/01/2023]. See the Terms and Conditions (https://onlinelibrary.wiley.com/terms-and-conditions) on Wiley Online Library for rules of use; OA articles are governed by the applicable Creative Commons License

Table 5. Stability data of various formulations at 5 °C.

Formulation	EE% (DOX)		EE% (PSC 833)/(TPGS 1000)		Particle size (nm)		Zeta potential (mV)	
	Day 0	Day 15	Day 0	Day 15	Day 0	Day 15	Day 0	Day 15
TPGS 1000-PM	–	–	*	*	235	247	−8.6	−7.7
DOX/TPGS 1000-PM	82.36	78.63	*	*	227	240	−9.7	−8.6
PSC 833-PM	–	–	69.82	65.93	246	256	−4.0	−4.3
DOX/PSC 833-PM	79.47	75.12	70.54	66.02	277	292	−5.5	−3.7

Possibly, some sort of copolymer swelling and/or hydration (in consequence of existence of the hydrophilic PEG parts in the micelles surfaces) might be responsible for this circumstance.[34] Results given in Table 5 demonstrates that the zeta potential of all PMs did not change considerably.

Conclusion

In this report, some fundamental work has been done concerning the development of an amphiphilic block copolymer based micelle drug delivery system for DOX. First of all four factors were chosen to control these experiments. FT-IR analysis confirmed that DOX was successfully loaded into PMs. After that, co-encapsulated DOX/PSC 833-PMs and DOX/TPGS 1000-PMs were prepared and characterized. Co-encapsulated all PMs showed high EE and DL, and small particle size. The EE values of DOX were 79.47 and 82.36% for DOX/PSC 833-PMs and DOX/TPGS 1000-PMs, respectively. In formulations containing two active agents, the entrapment efficiency of DOX was found to be higher in comparison with DOX-PM (78.98%) due to P-gp inhibitors. The micelle system produced here is successful because it has a high drug-loading capacity and thereby reduces the quantity of matrix materials for administration. In vitro experiments also showed that the co-encapsulated all PMs could release DOX in a controlled manner. It is apparent from this study that PMs exhibits an extended physical stability more than 15 days. The data obtained in this study have shown that two complementary active drugs might be associated with PMs using the nanoprecipitation method without any toxic organic solvent or severe experimental conditions. In addition a single delivery system that encapsulating two drugs in the same platform can lead to synchronized and controlled pharmacokinetics of each drug, resulting in improved drug efficacy, single formulation with improved solubility and bioavailability.

Acknowledgements

This work was supported by Research Fund of the Yildiz Technical University [Project Number: 2014-07-01-DOP04].

Conflict of Interest

The authors declare no conflict of interest.

Data Availability Statement

Research data are not shared.

Keywords: D-α-tocopherol Polyethylene Glycol 1000 Succinate · Doxorubicin · Drug Delivery · Micelles · Valspodar

[1] J. Wang, S. Li, Y. Han, J. Guan, S. Chung, C. Wang, D. Li, *Front. Pharmacol.* **2018**, *9*, DOI: 10.3389/fphar.2018.00202.
[2] H. K. Manjili, H. Malvandi, M. S. Mousavi, E. Attari, H. Danafar, *Artif. Cells, Nanomed., Biotechnol.* **2018**, *46*, 926–936.
[3] D. Wang, F. Luo, F. He, F. Lu, X. Tao, K. Song, J. Zhao, L. Chen, *J. Drug Delivery Sci. Technol.* **2021**, *66*, DOI: 10.1016/j.jddst.2021.102782.
[4] N. Ahmad, R. Ahmad, M. A. Alam, F. J. Ahmad, *Chem. Cent. J.* **2018**, *12*, DOI: 10.1186/s13065-018-0434-1.
[5] C. Yang, T. Wu, Y. Qi, Z. Zhang, *Theranostics*. **2018**, *8*, 464–485.
[6] M. Daga, I. A. M. de Graaf, M. Argenziano, A. S. M. Barranco, M. Loeck, Y. Al-Adwi, M. A. Cucci, F. Caldera, F. Trotta, G. Barrera, A. Casini, R. Cavalli, S. Pizzimenti, *Toxicol. in Vitro* **2020**, *65*, DOI: 10.1016/j.tiv.2020.104800.
[7] R. D. Al Bostami, W. H. Abuwatfa, G. A. Husseini, *Nanomaterials.* **2022**, *12*, DOI: 10.3390/nano12152672.
[8] O. Gökçe Kocabay, O. İsmail, *Int. J. Polym. Mater. Polym. Biomater.* **2021**, *70*, 328–337.
[9] Ö. Gökçe Kocabay, O. İsmail, *Rev. Roum. Chim.* **2018**, *63*, 1157–1167.
[10] O. Gökçe Kocabay, O. İsmail, *Polym. Sci.-A.* **2021**, *63*, 493–504.
[11] L. Azouz, F. Dahmoune, F. Rezgui, C. G'Sell, *Mater. Sci. Eng. C.* **2016**, *58*, 412–419.
[12] W. J. Kim, E. H. Lee, Y.-J. Kwon, S.-K. Ye, K. O. Kim, *RSC Adv.* **2022**, *12*, 18209–18214.
[13] Y.-F. Ding, J. Wei, S. Li, Y.-T. Pan, L.-H. Wang, R. Wang, *ACS Appl. Mater. Interfaces*. **2019**, *11*, 28665–28670.
[14] M. M. Lübtow, M. S. Haider, M. Kirsch, S. Klisch, R. Luxenhofer, *Biomacromolecules.* **2019**, *20*, 3041–3056.
[15] J. K. Ogunjobi, O. M. Balogun, *Sci. Rep.* **2021**, *11*, DOI: 10.1038/s41598-020-78533-6.
[16] C. Na, MSc Thesis, Department of Chemical and Biomolecular Engineering National University of Singapore, **2007**.
[17] M. Y. Nassar, H. I. El-Salhy, W. H. El-Shiwiny, G. Abdelaziz, R. El-Skiekh, *J. Inorg. Organomet. Polym. Mater.* **2022**, DOI: 10.1007/s10904-022-02498-4.
[18] G. Karakus, A. Ece, A. S. Yaglioglu, H. B. Zengin, M. Karahan, *Polym. Bull.* **2017**, *74*, 2159–2184.
[19] H. Yasin, B. Al-Taani, M. S. Salem, *Res. Pharm. Sci.* **2021**, *16*, 1–15.
[20] H. A. A. Enin, A. F. Alquthami, A. M. Alwagdani, L. M. Yousef, M. S. Albuqami, M. A. Alharthi, H. O. Alsaab, *Colloids Interfaces* **2022**, *6*, DOI: 10.3390/colloids6030049.
[21] X. Li, L. Wang, B. Wang, *Food Chem.* **2017**, *229*, 479–486.
[22] L. Zhang, Z. Chen, H. Wang, S. Wu, K. Zhao, H. Sun, D. Kong, C. Wang, X. Leng, D. Zhu, *RSC Adv.* **2016**, *6*, 54727–54737.
[23] S. O. Dozie-Nwachukwu, Y. Danyuo, J. D. Obayemi, O. S. Odusanya, K. Malatesta, W. O. Soboyejo, *Mater. Sci. Eng. C.* **2017**, *71*, 268–278.
[24] U. D. Shivhare, H. D. Rathod, V. B. Mathur, *Scholars Acad. J. Pharm.* **2013**, *2*, 365–372.
[25] C. H. Cavalcante, R. S. Fernandes, J. de Oliveira Silva, C. M. R. Oda, E. A. Leite, G. D. Cassali, I. Charlie-Silva, B. H. V. Fernandes, L. A. M. Ferreira,

© 2023 Wiley-VCH GmbH

A. L. B. de Barros, *Biomed. Pharmacother.* **2021**, *134*, DOI: 10.1016/j.biopha.2020.111076.
[26] J. Emami, M. Rezazadeh, M. Rostami, F. Hassanzadeh, H. Sadeghi, A. Mostafavi, M. Minaiyan, A. Lavasanifar, *Drug Dev. Ind. Pharm.* **2015**, *41*, 1137–1147.
[27] R. B. Mokhtari, T. S. Homayouni, N. Baluch, E. Morgatskaya, S. Kumar, B. Das, H. Yeger, *Oncotarget.* **2017**, *8*, 38022–38043.
[28] Z. Binkhathlan, PhD Thesis, Pharmaceutical Sciences of University of Alberta, **2011**.
[29] Y. H. A. Hussein, M. Youssry, *Materials.* **2018**, *11*, DOI: 10.3390/ma11050688.
[30] W. Hao, Y. Shen, D. Liu, Y. Shang, J. Zhang, S. Xu, H. Liu, *RSC Adv.* **2017**, *7*, 851–860.
[31] J. Y. Teo, W. Chin, X. Ke, S. Gao, S. Liu, W. Cheng, J. L. Hedrick, Y. Y. Yang, *Nanomedicine.* **2017**, *13*, 431–442.
[32] E. Akyol, S. Senol, *J. Mater. Sci.* **2018**, *53*, 14953–14963.
[33] L. M. Johnson, S. A. Krovi, L. Li, N. Girouard, Z. R. Demkovich, D. Myers, B. Creelman, A. Van der Straten, *Pharmaceutica* **2019**, *11*, DOI: 10.3390/pharmaceutics11070315.
[34] K. Rostamizadeh, M. Manafi, H. Nosrati, H. K. Manjili, H. Danafar, *New J. Chem.* **2018**, *42*, 5937–5945.
[35] J. Xu, S. Zhang, A. Machado, S. Lecommandoux, O. Sandre, F. Gu, A. Colin, *Sci. Rep.* **2017**, *7*, DOI: 10.1038/s41598-017-05184-5.
[36] C. Liu, Z. Wang, X. Wei, B. Chen, Y. Luo, *Acta Biomater.* **2021**, *131*, 314–325.
[37] R. Farajzadeh, Y. Pilehvar-Soltanahmadi, M. Dadashpour, S. Javidfar, J. Lotfi-Attari, H. Sadeghzadeh, V. Shafiei-Irannejad, N. Zarghami, *Artif. Cells, Nanomed., Biotechnol.* **2018**, *46*, 917–925.

Submitted: November 22, 2022
Accepted: January 10, 2023

© 2023 Wiley-VCH GmbH

23656549, 2023, 4, Downloaded from https://chemistry-europe.onlinelibrary.wiley.com/doi/10.1002/slct.202204543 by Yildiz Teknik University, Wiley Online Library on [25/01/2023]. See the Terms and Conditions (https://onlinelibrary.wiley.com/terms-and-conditions) on Wiley Online Library for rules of use; OA articles are governed by the applicable Creative Commons License